Astron. Astrophys. 248, 563–573 (1991)

ASTRONOMY AND ASTROPHYSICS

A *uvbyβ* survey of northern-hemisphere active binaries

II. The m_1 deficiency

A. Giménez[1], V. Reglero[2], E. de Castro[3] and M.J. Fernández-Figueroa[3]

[1] Laboratorio de Astrofísica Espacial y Física Fundamental, Instituto Nacional de Técnica Aeroespacial, E-28850 Torrejón de Ardoz (Madrid), Spain
[2] Departamento de Matemática Aplicada y Astronomía, Facultad de Matemáticas, Universidad de Valencia, E-46100 Burjasot, Valencia, Spain
[3] Departamento de Astrofísica, Facultad de Ciencias Físicas, Universidad Complutense, E-28040 Madrid, Spain

Received May 28, 1990; accepted January 30, 1991

Abstract. New photometric observations, using the *uvby* and Hβ systems of 72 northern-hemisphere active binaries are discussed in order to explain the main characteristics of their spectral light intensity distribution. Values of the parameter δm_1 range from 0.0 to 0.3 mag, which cannot be explained in terms of metal underabundance alone. The existence of some mechanism, responsible for such a colour-index anomaly, is thus suggested and is found to be in close relation with the involved degree of solar-type activity.

Key words: binary stars – RS CVn stars – stellar activity – *uvbyβ* photometry

1. Introduction

Active late-type binaries are the subject of an intense research at very different wavelength ranges because of their suitability as a primary source of information with respect to the actual physical mechanisms responsible for coronal and chromospheric activity, their evolution and dependence on stellar convection, rotation and magnetic fields. The currently adopted general picture is based in the emergence of magnetic flux tubes producing active regions "analogous" to those in the Sun with spots, active chromospheres and coronae. A review of these topics is given, e.g. by Byrne & Rodonò (1983) and Hartmann & Noyes (1987).

For this reasons, chromospherically active binaries have received much attention during the last few years from observers using astronomical satellites in the ultraviolet and X-ray ranges. But, ground-based photometric observations provide an important contribution to the understanding of the involved processes. In particular, it is now currently accepted that *uvby* photometry yields an excellent basis for the determination of effective temperatures and luminosity classes in late-type stars (Olsen 1984; Ardeberg & Lindgren 1985). In a previous paper, we have published a survey of 72 active binaries, of the RS CVn as well as other related types, in the northern hemisphere (Reglero et al. 1987), using *uvbyβ* photometry.

Send offprint requests to: V. Reglero

A preliminary presentation of astrophysical results from our four-colour photometry survey was made by Giménez et al. (1987). In the present paper, we discuss the main physical parameters that can be derived from the available data for separable systems and the location of active binaries in the m_1 and c_1 versus $(b-y)$ diagrams with respect to normal stars.

2. The observations

All measurements were collected by means of the two-channel photoelectric photometer attached to the 1 m JKT reflecting telescope of the Observatorio del Roque de los Muchachos (La Palma, Canary Islands). Extinction corrections were applied using coefficients determined for each individual night and particular attention was paid to the transformation equations from the instrumental to the standard *uvby* and Hβ systems. The observations were made during three campaigns devoted to the project in May 1985, November 1985, and March 1986. A large number of standard stars, carefully selected to provide an adequate coverage in the different colour indices, was observed and all data reductions were made in a completely homogeneous way, following a procedure similar to that described by Grønbech et al. (1976). Further details are given by Reglero et al. (1987).

In Table 1, the complete list of observed objects is given with identification in different source catalogues and, in particular, in the latest compilation by Strassmeier et al. (1988) at column 5. Known visual binaries are marked by an asterisk in column 6. In Table 2, average magnitudes and colour indices for the target objects are given as derived from the original data published by Reglero et al. (1987). Observations within eclipse or doubtful data obtained during nights with too large extinction were not included for the computation of these average values. The number of individual measurements taken into account is given in the last column of Table 2. Known visual binaries, indicated in Table 1, have been corrected for the light contribution from the non-active companion when this was found necessary.

Mean errors for the tabulated colours and magnitudes of individual stars are difficult to estimate due to the presence of migrating-wave photometric variations but average values are in agreement with the internal accuracies given by Reglero et al.

Table 1. Observed stars and identifications

No.	Name	HR	HD/HDE	Str.	Vis.	Gr.	ΔV
1	ζ And	215	4502	7		3	—
2	33 Psc	3	28	1		3	—
3	BD Cet		1833	4		3	0.10
4	13 Cet	142	3196	5	*	1	0.00
5	AY Cet	373	7672	11		3	0.22
6	UV Psc		7700	12		1	0.05
7	AR Psc		8357	15		1	0.08
8	LX Per			24		2	0.08
9	UX Ari		21242	26		2	0.15
10	V711 Tau	1099	22468	27	*	2	0.22
11	EI Eri		26337	31		2	0.19
12	RZ Eri		30050	38		3	0.07
13	TW Lep		37847	44		3	0.32
14	BM Cam	1623	32357	40		3	0.14
15	CQ Aur		250810	48		3	0.12
16	SV Cam		44982	53		1	0.08
17	VV Mon			54		2	0.12
18	SS Cam			56		2	0.13
19	AR Mon		57364	57		3	—
20	σ Gem	2973	62044	60		3	0.15
21	54 Cam	3119	65626	61		2	0.05
22	RU Cnc			65		2	0.1
23	RZ Cnc		73343	66		3	0.05
24	GK Hya			63		2	—
25	TY Pyx		77137	67		2	0.04
26	WY Cnc			68		1	0.035
27	XY UMa			69		1	0.11
28	DH Leo		86590	73		1	0.15
29	DM UMa			75		1	0.32
30	RW UMa			80		2	0.10
31	DQ Leo	4527	102509	81		3	0.03
32	ξ UMa	4374	98230	76	*	1	—
33	DK Dra	4665	106677	83		3	0.28
34	AS Dra		107760	84		1	0.05
35			108102	85		1	0.04
36	UX Com			87		2	0.10
37	RS CVn		114519	89		2	0.22
38	BH CVn	5110	118216	91		2	—
39	SS Boo			98		2	0.20
40	GX Lib		136905	100		3	0.1
41	RT CrB		139588	103		2	—
42	RS UMi			105		2	—
43	TZ CrB	6063	146361	107	*	1	0.05
44	WW Dra		150708	109	*	2	0.10
45	ε UMi	6322	153751	110	*	3	—
46	V792 Her		155638	111		3	0.15
47		6469	157482	113		2	0.04
48	DR Dra		160537	115		3	0.12
49	Z Her		163930	117		2	0.04
50	MM Her		341475	118		2	0.23
51	V815 Her		166181	122		1	0.10
52	AW Her		348635	125		2	—
53	o Dra	7125	175306	127	*	3	0.034
54	V775 Her		175742	129		1	0.11
55	V478 Lyr		178450	131		1	0.033
56	V1762 Cyg	7275	179094	132		3	0.3
57		7428	184398	136		3	—

Table 1 (continued)

No.	Name	HR	HD/HDE	Str.	Vis.	Gr.	ΔV
58	V1764 Cyg		185151	137		3	0.09
59			185510	138		3	0.20
60			205249	149		3	0.14
61	AD Cap		206046	150		1	—
62	42 Cap	8283	206301	151		2	—
63	CG Cyg			142		1	0.11
64	ER Vul		200391	144		1	0.04
65	RT Lac		209318	153		2	0.17
66	AR Lac	8448	210334	155		2	0.13
67	HK Lac		209813	154		3	0.25
68	V350 Lac	8575	213389	157		3	—
69	SZ Psc		219113	164		2	0.213
70	RT And			163		1	0.06
71	λ And	8961	222107	166		3	0.28
72	II Peg		224085	168		2	0.43

Notes
Str.: Catalogue number from Strassmeier et al. 1988.
*: Systems with close visual companion.
Gr.: Stars belonging to groups 1, 2 and 3 as defined in text.

Table 2. Average photometric data

No.	Name	V	$b-y$	m_1	c_1	β	N
1	ζ And	4.13	0.681	0.464	0.315	2.564	8
2	33 Psc	4.64	0.625	0.455	0.364	2.552	4
3	BD Cet	7.97	0.716	0.439	0.338	2.542	2
4	13 Cet	5.22	0.358	0.185	0.371	2.619	4
5	AY Cet	5.47	0.560	0.289	0.323	2.549	4
6	UV Psc	9.15	0.460	0.229	0.291	2.573	4
7	AR Psc	7.25	0.533	0.271	0.260	2.522	4
8	LX Per	8.15	0.488	0.233	0.337	2.558	4
9	UX Ari	6.47	0.579	0.278	0.274	2.540	4
10	V711 Tau	5.87	0.579	0.293	0.266	2.526	4
11	EI Eri	7.18	0.450	0.204	0.322	2.574	2
12	RZ Eri	7.81	0.431	0.181	0.764	2.691	6
13	TW Lep	7.57	0.687	0.352	0.265	2.565	4
14	BM Cam	6.17	0.706	0.437	0.287	2.562	8
15	CQ Aur	9.07	0.577	0.237	0.419	2.609	12
16	SV Cam	9.19	0.440	0.210	0.343	2.579	8
17	VV Mon	9.47	0.533	0.223	0.296	2.582	6
18	SS Cam	10.16	0.511	0.267	0.324	2.615	2
19	AR Mon	8.75	0.690	0.353	0.371	2.599	2
20	σ Gem	4.25	0.697	0.522	0.283	2.566	8
21	54 Cam	6.51	0.404	0.194	0.412	2.608	8
22	RU Cnc	10.07	0.441	0.171	0.406	2.624	4
23	RZ Cnc	8.80	0.759	0.519	0.226	2.572	10
24	GK Hya	9.33	0.473	0.200	0.339	2.590	4
25	TY Pyx	6.84	0.433	0.229	0.372	2.603	1
26	WY Cnc	9.42	0.448	0.232	0.278	2.572	6
27	XY UMa	9.65	0.548	0.294	0.306	2.558	4
28	DH Leo	7.91	0.564	0.329	0.283	2.567	10
29	DM UMa	9.61	0.652	0.407	0.182	2.532	6
30	RW UMa	10.17	0.432	0.174	0.370	2.614	4
31	DQ Leo	4.54	0.356	0.195	0.704	2.681	14
32	ξ UMa	4.82	0.378	0.175	0.297	2.590	14
33	DK Dra	6.31	0.713	0.503	0.279	2.569	6
34	AS Dra	8.07	0.470	0.238	0.276	2.558	9

Table 2 (continued)

No.	Name	V	$b-y$	m_1	c_1	β	N
35	HD 108102	8.12	0.348	0.170	0.335	2.625	8
36	UX Com	10.02	0.543	0.290	0.268	2.572	4
37	RS CVn	8.08	0.409	0.155	0.382	2.607	20
38	BH CVn	4.95	0.274	0.155	0.652	2.678	14
39	SS Boo	10.28	0.526	0.199	0.288	2.561	12
40	GX Lib	7.32	0.650	0.351	0.397	2.549	6
41	RT CrB	10.21	0.459	0.201	0.367	2.558	17
42	RS UMi	10.40	0.513	0.188	0.342	2.553	4
43	TZ CrB	5.57	0.382	0.174	0.319	2.597	12
44	WW Dra	8.29	0.433	0.195	0.351	2.596	6
45	ε UMi	4.23	0.567	0.330	0.367	2.576	3
46	V792 Her	8.11	0.589	0.276	0.329	2.568	10
47	HD 157482	5.57	0.431	0.212	0.430	2.611	10
48	DR Dra	6.67	0.667	0.389	0.333	2.560	4
49	Z Her	7.23	0.403	0.172	0.414	2.620	2
50	MM Her	9.58	0.544	0.243	0.325	2.573	12
51	V815 Her	7.78	0.470	0.220	0.299	2.568	10
52	AW Her	9.81	0.526	0.197	0.346	2.590	12
53	o Dra	4.65	0.730	0.465	0.335	2.571	4
54	V775 Her	8.06	0.565	0.348	0.297	2.532	4
55	V478 Lyr	7.71	0.478	0.253	0.297	2.564	10
56	V1762 Cyg	5.99	0.689	0.428	0.320	2.551	10
57	HD 184398	6.50	0.735	0.393	0.327	2.585	8
58	V1764 Cyg	7.85	0.829	0.378	0.285	2.588	10
59	HD 185510	8.59	0.776	0.285	0.254	2.559	7
60	HD 205249	7.82	0.638	0.429	0.311	2.554	8
61	AD Cap	9.67	0.585	0.291	0.263	2.529	4
62	42 Cap	5.19	0.418	0.204	0.371	2.588	4
63	CG Cyg	9.99	0.539	0.287	0.243	2.521	4
64	ER Vul	7.34	0.393	0.185	0.329	2.587	6
65	RT Lac	8.92	0.700	0.364	0.333	2.542	6
66	AR Lac	6.14	0.477	0.235	0.329	2.577	6
67	HK Lac	6.93	0.662	0.373	0.280	2.553	4
68	V350 Lac	6.46	0.728	0.503	0.287	2.559	4
69	SZ Psc	7.33	0.538	0.253	0.278	2.573	2
70	RT And	8.97	0.374	0.166	0.342	2.601	6
71	λ And	3.83	0.619	0.328	0.383	2.539	6
72	II Peg	7.46	0.638	0.340	0.323	2.512	6

(1987), i.e. about ± 0.012, 0.005, 0.008, 0.008 and 0.005 in V, $(b-y)$, m_1, c_1, and β respectively.

3. Photometric calibrations

The intermediate band photometric *uvby* system, as defined by Strömgren (1966), was in principle limited to stars of spectral type earlier than that of the Sun. Extended calibrations, as for the *F*-type stars (Crawford 1975), are not yet available for spectral types later than about G2. Nevertheless, several authors have already attempted to break this barrier and have carried out a systematic study of late-type stars in the *uvby* system like, Olson (1974) and the above mentioned Ardeberg & Lindgren (1985). The first, though preliminary, quantitative calibration towards the use of *uvby* photometry in the analysis of the physical parameters of cool stars was published by Olsen (1984) for main-sequence stars down to M2. Moreover, Olsen located the average position of giants and subgiants in the m_1 and c_1 versus $(b-y)$ diagrams. The parameter $\delta m_1 = m_1(\text{Hyades}) - m_1(\text{obs})$, is currently used as an indicator of stellar metallicity and, though the $c_1-(b-y)$ diagram is very sensitive to luminosity class, the $m_1-(b-y)$ plot is not significantly dependent on $\log g$ effects for stars close to the Main Sequence. Already Nelles et al. (1985) and Schuster & Nissen (1989) showed this fact and proposed new relations between m_1 and metallicity.

Nevertheless, we have to take into account that the observed colour indices in Table 2 correspond to the combination of two stars forming a binary system. In order to interpret the results of the present survey, we have studied the effects of binarity, for the *uvby* system, in the observed combined colours. A discussion of the main results is given by Giménez et al. (1986b and 1987). Summarizing, it was shown that the combination of two main sequence stars produces a point located also within the main sequence with a relative position, with respect to the individual components, depending on the luminosity ratio. Obviously, the combined colours coincide with those corresponding to the primary component in the cases of luminosity ratio 1 and 0, the departure being largest for values around 0.7. Combination with subgiant stars give much more difficult to interpret results, but, in general, reproduce the position of metal-deficient dwarfs in the

m_1 versus $(b-y)$ diagram and slightly evolved stars in the c_1 versus $(b-y)$ diagram. Real metal-deficient dwarfs should be easy to discriminate from these two diagrams in light of their position in the c_1 versus $(b-y)$ plane.

The most interesting information about the stars under study is provided by their location in the m_1 and c_1 versus $(b-y)$ diagrams with respect to the corresponding calibrations for normal main-sequence stars. In order to consider the position of our active binaries in the mentioned diagrams we have divided the sample in three distinct groups according to their evolutionary status. Group 1 contains systems with both components within the main sequence. Group 2 includes those binaries with at least one of the components classified as subgiant and, finally, group 3 corresponds to those with at least one giant component. For each of the systems in the survey, the group to which it belongs has been included in Table 1 (column 7). In all cases, luminosity classes given in the literature have been used (mainly from Strassmeier et al. 1988), except for DM UMa for which a main-sequence classification is in better agreement with available photometric data.

In Figs. 1 and 2 the corresponding positions in the $m_1-(b-y)$ and $c_1-(b-y)$ planes, respectively, are plotted with differ-

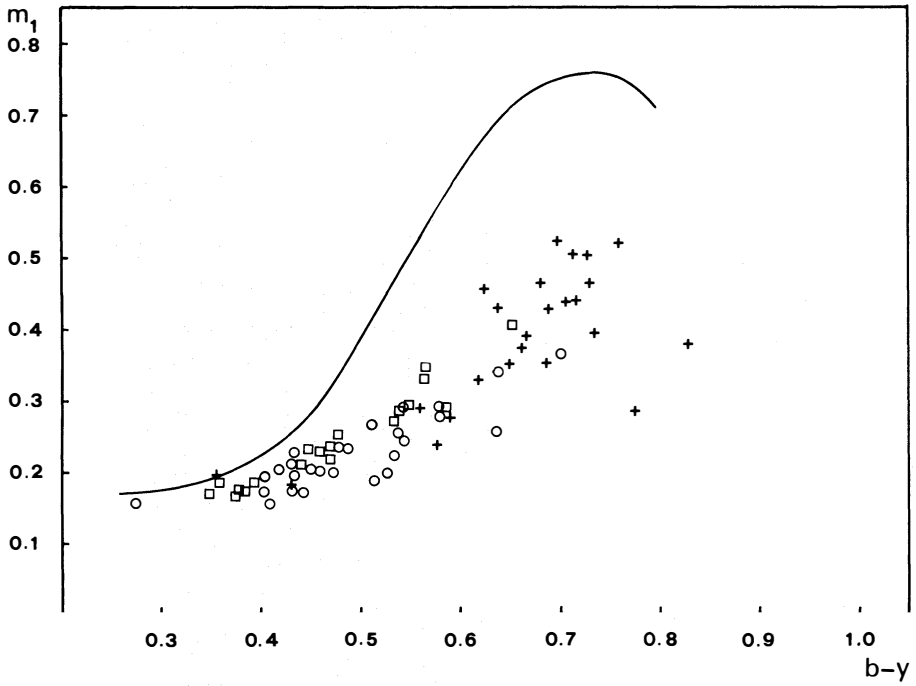

Fig. 1. The $m_1-(b-y)$ diagram for the program stars. The curve represents calibration for ZAMS. Symbols denote groups defined in text as group 1 (□), group 2 (○) and group 3 (+)

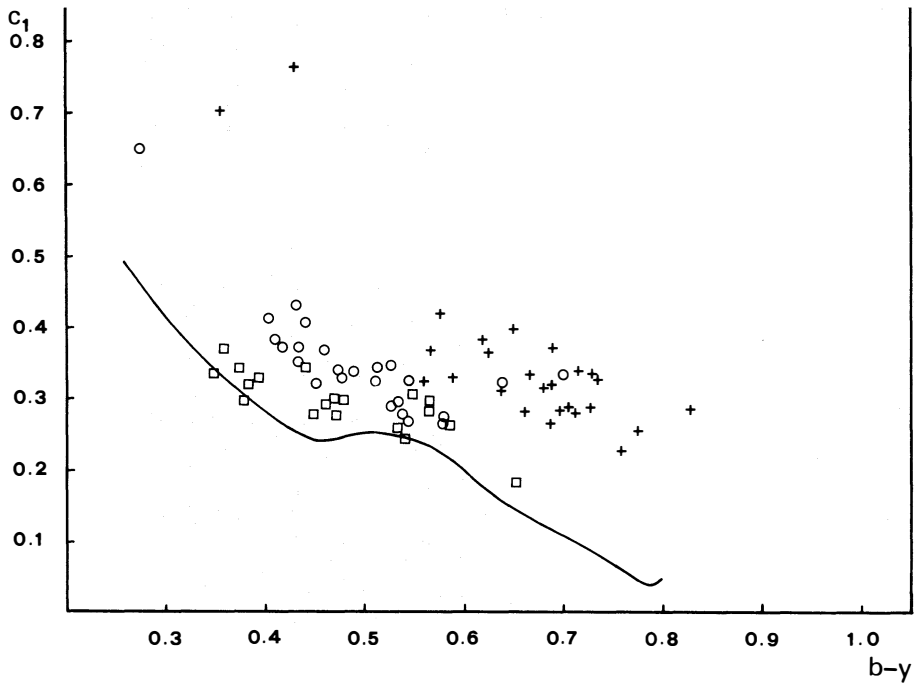

Fig. 2. The $c_1-(b-y)$ diagram for the program stars. The curve represents calibration for ZAMS. Symbols denote groups defined in text as group 1 (□), group 2 (○) and group 3 (+)

ent symbols for each group: (□) for Group 1, (○) for Group 2 and (+) for Group 3. No correction for interstellar reddening has been applied due to the expected proximity of the observed systems. We assume that the effects of the interstellar medium within 100 pc are negligible and binaries with giant components (Group 3) may be affected by reddening. Continuous lines denote the standard relations for unevolved normal stars as given by Crawford (1975) and Olsen (1988) for F-type stars and Olsen (1984) for the later types. It is evident, from Fig. 2, that the c_1 index permits the separation of luminosity classes and the behavior of the surveyed active binaries is comparable to that of normal individual stars with respect to this index. On the other hand, Fig. 1 shows a systematic deficiency of m_1, too large to be explained in terms of metal underabundance or evolution. We discuss the astrophysical significance of these results in next section.

4. Astrophysical discussion

The first point that we wanted to delucidate at the beginning of this project was how much are Strömgren indices actually affected by chromospheric activity. For this purpose, we have plotted in Figs. 3 and 4 the corresponding values of δm_1 and δc_1, given in Table 3, versus the standard index $(b-y)$, for binaries which

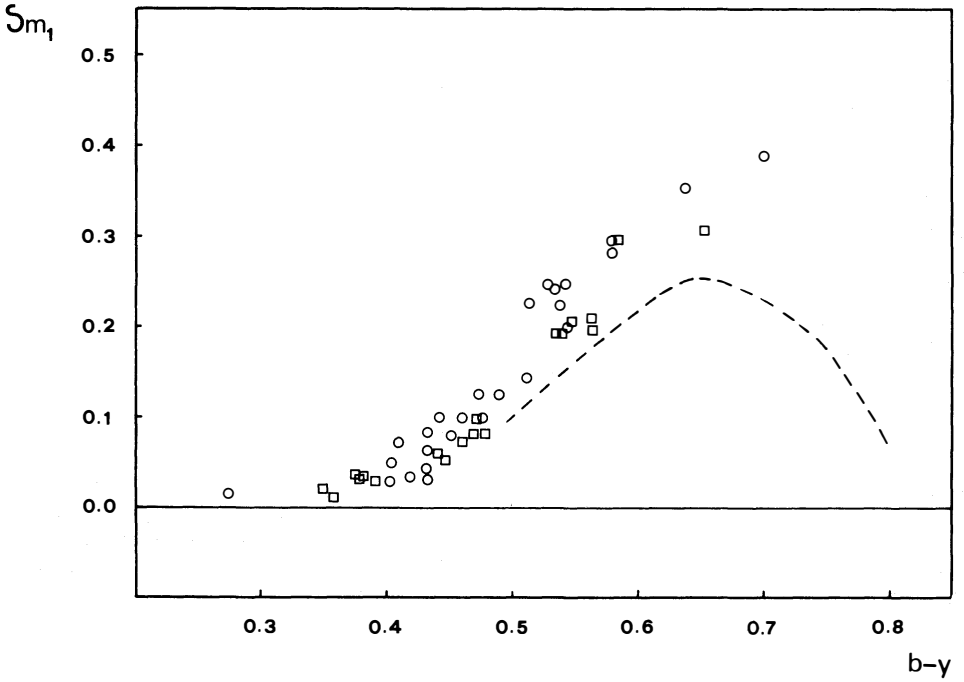

Fig. 3. The $\delta m_1-(b-y)$ diagram for program stars belonging to group 1 and 2

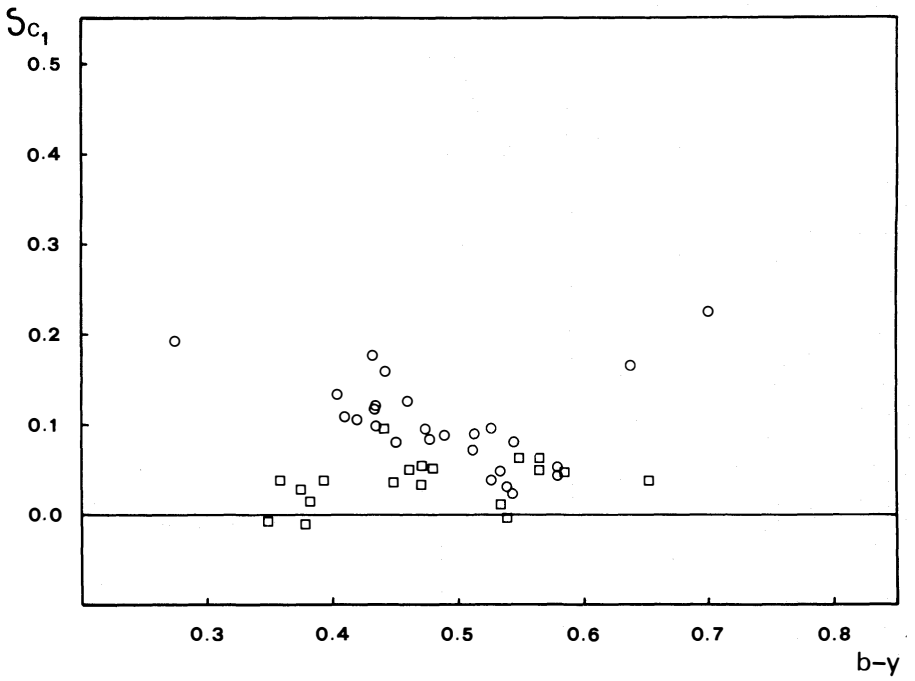

Fig. 4. The $\delta c_1-(b-y)$ diagram for program stars belonging to group 1 and 2

Table 3. Average temperatures and colour excesses

No.	Name	T_{eff}	δm_1	δc_1
4	13 Cet	6020	0.01	0.04
6	UV Psc	5400	0.07	0.05
7	AR Psc	4870	0.19	0.01
8	LX Per	5300	0.12	0.09
9	UX Ari	4690	0.30	0.05
10	V711 Tau	4690	0.28	0.04
11	EI Eri	5460	0.08	0.08
16	SV Cam	5510	0.06	0.10
17	VV Mon	4870	0.24	0.05
18	SS Cam	4950	0.14	0.07
21	54 Cam	5700	0.03	0.13
22	RU Cnc	5500	0.10	0.16
24	GK Hya	5340	0.13	0.10
25	TY Pyx	5540	0.03	0.12
26	WY Cnc	5470	0.05	0.04
27	XY UMa	4810	0.21	0.06
28	DH Leo	4750	0.21	0.05
29	DM UMa	4430	0.31	0.04
30	RW UMa	5550	0.08	0.12
32	ξ UMa	5800	0.03	−0.01
34	AS Dra	5350	0.09	0.04
35	HD 108102	6060	0.02	−0.01
36	UX Com	4820	0.20	0.02
37	RS CVn	5670	0.07	0.11
38	BH CVn	6560	0.02	0.20
39	SS Boo	4890	0.25	0.04
41	RT CrB	5410	0.10	0.13
42	RS UMi	4940	0.23	0.09
43	TZ CrB	5830	0.03	0.01
44	WW Dra	5540	0.06	0.10
47	HD 157482	5560	0.04	0.18
49	Z Her	5710	0.05	0.13
50	MM Her	4820	0.25	0.08
51	V815 Her	5350	0.10	0.06
52	AW Her	4890	0.25	0.10
54	V775 Her	4750	0.20	0.06
55	V478 Lyr	5310	0.08	0.05
61	AD Cap	4670	0.30	0.05
62	42 Cap	5620	0.03	0.11
63	CG Cyg	4840	0.19	0.00
64	ER Vul	5740	0.03	0.04
65	RT Lac	4270	0.39	0.23
66	AR Lac	5320	0.10	0.08
69	SZ Psc	4850	0.23	0.03
70	RT And	5870	0.04	0.03
72	II Peg	4480	0.35	0.17

belong to our Groups 1 (□) and 2 (○). Giants are not included in further discussion due to the lack of reliable calibrations and correction for reddening. These parameters are defined as,

$\delta m_1 = m_1$(standard line) $- m_1$(observed)

$\delta c_1 = c_1$(observed) $- c_1$(standard line).

Two things can be clearly seen from these plots which confirm the general view derived from Figs. 1 and 2 for all the binaries in our sample. First, the δc_1 parameter does actually discriminate between different degrees of evolution for active stars and, secondly, there is a large deviation of m_1 from the expected main-sequence values which cannot be due to metal deficiency alone. In terms of standard calibrations, the observed values of δm_1 would represent metal deficiencies up to −6 dex in [Fe/H] with respect to the solar value – using the calibration by Olsen (1984) and δm_1 up to 0.3. Furthermore, a distinct linear relation is found, independent of evolution, between δm_1 and $(b-y)$. To explain this relation we have to accept, either a systematic error in the standard calibration or a real difference of the atmospheres of active binaries.

We are quite confident on the calibration curves for the zero-age main sequence because of the different checks carried out for a sample of non-active stars, standard stars and non-binary slightly-active stars (Fabregat 1989). On the other hand, chromospheric activity is expected to fill-in the core of metallic lines in such a way that the observed colours would correspond to metal deficient dwarfs. The effect would obviously be strongly dependent on the relative importance of the continuum and thence the detected dependence on temperature or, for this matter, $(b-y)$.

In order to check for the effect of luminosity class, since no reliable photometric calibration is available for subgiants, we have plotted in Fig. 3, as an indication, the limit position corresponding to normal giants (dashed curves) and that for the zero-age main-sequence stars (continuous line) which, of course, coincides with the zero line of the ordinates. Estimations by Bond (1980) have been used to compute the expected position for giants. These curves, clearly confirm the above given results, showing that a problem in the definition of the zero-age main sequence cannot explain the observed linear trend.

Estimations of effective temperatures, for each binary system, were done using the equations by Olsen (1984):

$$\log T_{eff} = -0.416(b-y)+3.924 \quad \text{for} \quad 0.35 < b-y < 0.51$$

$$\log T_{eff} = -0.341(b-y)+3.869 \quad \text{for} \quad 0.51 < b-y < 0.98$$

Obviously, the obtained values correspond to an average of both components, the result being closer to the hotter star depending on the luminosity ratio. The lack of further available information for many systems makes these values important for other research works. For the few cases with $(b-y)$ smaller than 0.40, the standard calibration by Saxner & Hammarback (1985) was also calculated in terms of the β index and the average of the two methods was adopted though discrepancies were always below 100 K. We should point out that negligible effects are to be expected in the $(b-y)$ index due to spot coverage of the stellar surface since spots are essentially dark (relative luminosities being proportional to the forth power of the temperature) and, therefore, observed indices correspond to the temperature of the non-spotted surface sections. Results are given in Table 3 for all binaries which belong to groups 1 and 2. Temperatures are probably only slightly underestimated in the case of subgiants.

5. The case of separable systems

Throughout this paper, we have only used the combined colours of a sample of active binaries. Nevertheless, we are well aware of the fact that, in most cases, only one of the components – in fact the cooler one – does show chromospheric and coronal activity.

In order to check the physical reality of the results commented in the previous sections, we have analyzed in more detail

a few systems for which it is possible to separate the light contribution of each of the components. There are two possibilities: either the light curve shows total eclipses, during which the colours of the eclipsing star can be directly measured, or both components are identical. The best example of the first case is RS CVn itself and a throughout spectroscopic and photometric study of this system has been published recently (Reglero et al. 1990), but several other cases are found within our sample: CQ Aur, RU Cnc, AW Her and RW UMa. Individual colours derived for each of the components of these binaries, including RS CVn, are given in Table 4. Examples of the second mentioned case are TZ CrB, discussed in some detail by Giménez et al. (1986a), HD 108102, and possibly TY Pyx. Obviously, colours given in Table 2 are valid for each of the components of these latter binaries.

As in the case of RS CVn (Reglero et al. 1990), reddening and distances can be estimated using the non-active star, so that absolute magnitudes of the isolated active star can be determined as well as the effective temperature of each of the components. Further interesting parameters, like stellar radii and masses, can be derived from the analysis of both the light and radial velocity curves. Masses and radii given by Popper (1990) are listed in Table 5. Observed colour indices for the primary components allow us to estimate interstellar reddening and then the surface temperatures of the two components determined from the corrected colour indices. From all these parameters it is immediate to

Table 4. Systems with separable components

No.	Name	Component	V	$b-y$	m_1	c_1	δm_1	δc_1
15	CQ Aur	Combined	9.07	0.577	0.237	0.419		
		Hotter	10.50	0.327	0.146	0.553	0.04	0.18
		Cooler	9.41	0.685	0.355	0.384	0.39	0.27
22	RU Cnc	Combined	10.07	0.441	0.171	0.406		
		Hotter	10.59	0.335	0.136	0.479	0.05	0.12
		Cooler	11.07	0.635	0.352	0.254	0.34	0.09
30	RW UMa	Combined	10.17	0.432	0.174	0.370		
		Hotter	10.48	0.365	0.158	0.393	0.04	0.08
		Cooler	11.68	0.662	0.352	0.344	0.38	0.21
37	RS CVn	Combined	8.08	0.409	0.155	0.382		
		Hotter	8.59	0.303	0.127	0.419	0.05	0.01
		Cooler	9.16	0.610	0.333	0.293	0.31	0.11
52	AW Her	Combined	9.81	0.526	0.197	0.346		
		Hotter	10.34	0.462	0.166	0.377	0.14	0.14
		Cooler	10.84	0.636	0.289	0.302	0.40	0.14

Table 5. Properties of the components

	V_0	$(b-y)_0$	m_0	c_0	$H\beta$	$E(b-y)$	δm_0	δc_0	$(B-V)_0$	[Fe/H]
RU Cnc										
h	10.39	0.289	0.150	0.470	2.656	0.046	0.026	0.065	0.44	−0.1 2
c	10.87	0.589	0.366	0.245	2.560		0.267	0.034	0.95	−1.1 2
RW UMa										
h	10.32	0.328	0.169	0.386	2.634	0.037	0.017	0.028	0.50	0.0 2
c	11.52	0.625	0.363	0.337	2.540		0.308	0.167	1.00	−1.5 2
AW Her										
h	9.82	0.378	0.191	0.360	2.603	0.084	0.020	0.064	0.60	0.0 2
c	10.32	0.552	0.314	0.285	2.565		0.199	0.044	0.88	−1.0 2

Table 5 (continued)

	F_V	T	R^a	M_V	d	M_{bol}	BC	m^a	log g	Sp
RU Cnc										
h	3.805	6470	2.3	2.5	380	2.3	−0.2	1.46	3.88	F5IV
	34	60	3	3	50	3	4	7	6	
c	3.644	4660	5.2	3.0		2.0	−1.0	1.47	3.17	K1IV
	26	100	2	3		1	4	7	3	
RW UMa										
h	3.784	6250	2.31	2.70	330	2.48	−0.2	1.56	3.91	F8IV
	34	60	2	15	30	5	2	5	2	
c	3.625	4530	4.24	3.90		2.56	−1.3	1.49	3.54	K1IV
	26	100	2	15		10	2	6	2	
AW Her										
h	3.757	5920	2.4	2.9	240	2.6	−0.3	1.25	3.78	G0V
	34	60		2	20	1	2	13	5	
c	3.664	4800	3.6	3.4		2.7	−0.7	1.33	3.45	K1IV
	26	100		2		1	2	10	4	

[a] Assumed values from Popper 1990.

calculate absolute bolometric magnitudes and surface gravities, log g, as indicated in the same Table 5.

On the other colour indices, corrected for reddening, permit us to estimate M_V as given by,

$$M_V = 42.36 - 10\,F_V(b-y) - 5\log R,$$

for the primary components and the observed V luminosity ratios the corresponding values for the active secondaries. Bolometric corrections are obviously defined by M_V and M_{bol}. Finally, distances to the binary systems are evaluated from the results for the non-active primary stars.

CQ Aur is not included in our discussion of physical parameters due to the lack of a reliable calibration for highly evolved stars. An inspection of the results for the other binary components lead to several conclusions. The derived reddenings are in good agreement with expected values for the given distances and position in the galaxy. Global physical parameters for the component stars are found to be also in good agreement with previous results by Popper (1990) as well as with standard evolutionary models as shown in Fig. 5. Adopted models are described by Claret & Giménez (1989) for an initial chemical composition $(X, Z) = (0.70, 0.02)$ and mixing-length ratio of 2.0. Particular attention should be paid to the case of RW UMa for which the radiative and geometrical properties of the component stars do not fit with each other. Though the other systems also show a systematic effect, the case of RW UMa offers a much better determination of the geometrical parameters. Our results confirm the previous finding by Popper (1990) and is clearly seen in Table 5 through the computed B.C. Furthermore a lower than expected temperature for both components of RW UMa is shown in Fig. 5.

Besides the above commented discussion of the physical parameter, the main purpose of separating the component stars is nevertheless to check the linear trend observed for the combined light in the δm_1 parameter as a function of $(b-y)$ (Fig. 3). It is worth noticing that the apparent underabundance in metals, as derived from the observed δm_1 values and the calibration by

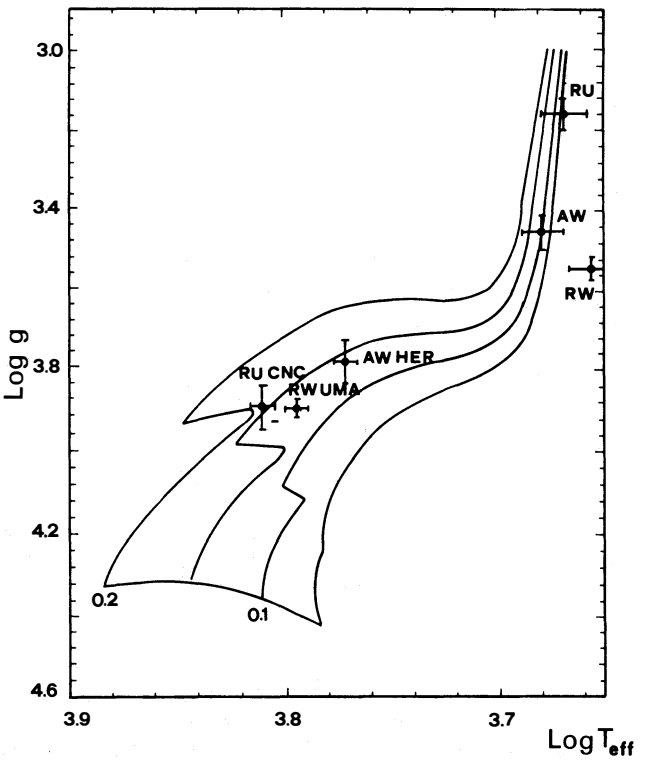

Fig. 5. Evolutionary tracks for the individual components in the separable systems RU Cnc, RW Uma AW Her and chemical composition $(X, Z) = (0.70, 0.20)$. The actual positions according to computed values in Table 5 are indicated with error bars. Numbers on tracks denote $\log(m/M_\odot)$

Nissen et al. (1987), occurs mainly for the cooler active components and not for the non-active primaries in contradiction with a chemical explanation of the effect according to a common origin hypothesis. In Fig. 6, we have plotted the position, in the

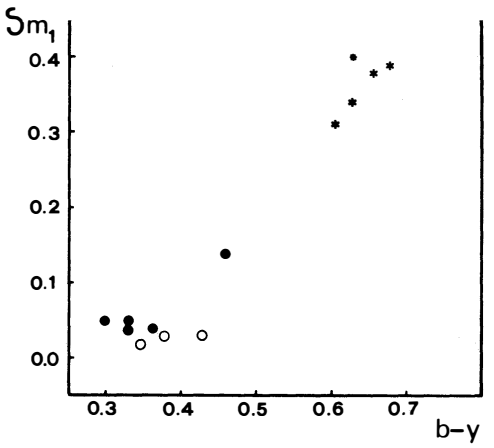

Fig. 6. The $\delta m_1 - (b-y)$ diagram for the individual components in the separable systems. Hot stars are denoted by filled circles and cool stars by asterisks. Open circles show the positions of systems with almost identical components

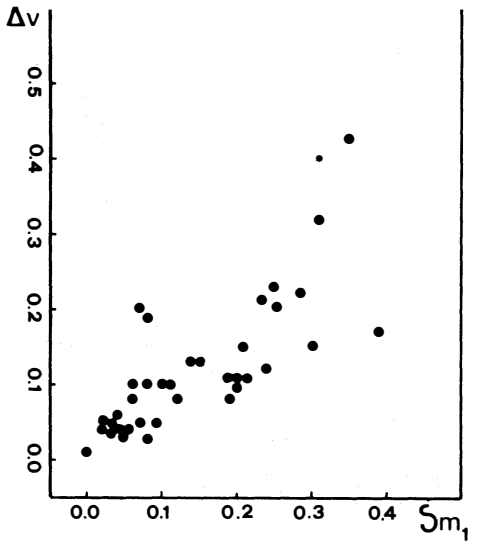

Fig. 7. Relation between amplitudes of outside eclipse variations ΔV and m_1 deficiency δm_1 for the combined light of systems which belong to groups 1 and 2. The cool component of RS Cvn is shown by an asterisk

$\delta m_1 - (b-y)$ plane, of the individual stars as indicated by data in Table 4 together with the position corresponding to the combined light for those systems with almost identical components. The same trend observed in Fig. 3 is clearly shown, thus supporting the results obtained in the previous section.

6. Conclusion

In order to show that, in fact, an important contribution to the observed m_1 deficiency may be due to some degree of stellar activity, we have plotted, in Fig. 6, the amplitude of the light variations outside of eclipse (the so-called migrating wave) versus the obtained value of δm_1 for stars in Groups 1 and 2. The amplitude of the light variations is known to be related to the surface coverage by spots and this depends on the degree of solar-type activity. We have adopted maximum values given mainly by Strassmeier et al. (1988) and included in column 8 of Table 1. Though the scatter is certainly large, due to the several parameters involved, the comparison of different epochs of activity and, again, the use of combined light instead of isolated active stars, a certain correlation is shown. In the case of RS CVn, we have also plotted the value corresponding to the isolated active component as given by Reglero et al. (1990).

Giampapa et al. (1979) compared measurements of the quiet solar photosphere and active solar regions in the *uvby* system showing that the effect of the active regions was to decrease the "apparent" metal abundance derived from the m_1 index in around 35%. On the other hand, it has been suggested by Petersen (1982), that chromospheric activity may affect the photometric indices by filling-in the core of strong non-magnetic lines as a result of non-thermal heating in the lower chromosphere. Finally, in a recent paper, Basri et al. (1989) have shown that activity in late-type main-sequence stars produce in fact a perturbation to the line profiles through pseudoemission features and broader wings but shallower cores.

In the case of W UMa-type binaries, Rucinski (1981) observed through the analysis of *uvby* photometry of the combined light, the most positive values of δm_1 and largest ultraviolet excesses for systems having the shortest periods at a given spectral type. He also noted that the reddening-corrected values of δc_1 were about zero with only slightly positive values in the case of systems with the earliest spectral types, which indicates just a slight evolutionary advance. Nevertheless, the possibility of intrinsic excesses in c_1 is still open in face of the found traces of correlation between δc_1 and δm_1 for the least evolved systems. A plot of the values given in Table 3 shows no significant dependence between δc_1 and δm_1.

We can then summarize the results obtained in this paper in the following: stellar activity does affect *uvby* indices in the sense that m_1 is smaller than for normal stars while c_1 remains practically unaltered, m_1 deficiency is correlated to the degree of activity and effective temperatures can be estimated from *uvby* indices for active late-type stars with an acceptable degree of confidence. The case of separable systems discussed in Sect. 5 shows strongly different m_1-deficiencies between hot and cool components, or active and normal components, thus supporting the relation of δm_1 with activity rather than with metal underabundancy.

Acknowledgements. The JKT, on the island of La Palma, is operated by the Royal Greenwich Observatory at the Spanish Roque de los Muchachos Observatory of the Instituto de Astrofísica de Canarias. We want to express our gratitude to the observatory staff for their help during the observations. Dr. E.H. Olsen is gratefully acknowledged for his comments during the preparation of the first draft. This work has been supported by the Spanish Comisión Interministerial de Ciencia y Tecnolgía (PB87-0235 and PB86-0536).

References

Ardeberg A., Lindgren H., 1985, in: Calibration of Fundamental Stellar Quantities, eds. D.S. Hayes et al., Reidel, Dordrecht, p. 509

Basri G., Wilcots E., Stout N., 1989, PASP 101, 528
Bond H.E., 1980, ApJS 44, 517
Byrne P.D., Rodonò M., 1983, in: Activity in Red Dwarf Stars, eds. P.D. Byrne, M. Rodonò, IAU Coll. No. 71, Reidel, Dordrecht
Claret A., Gimenez A., 1989, A&AS 81, 1
Crawford D.L., 1975, AJ 80, 955
Fabregat J., 1989, Ph.D. Thesis. Universidad de Valencia
Giampapa M.S., Worden S.P., Gilliam L.B., 1979, ApJ 229, 1143
Giménez A., Ballester J.M., Reglero V., Fernández-Figueroa M.J., de Castro E., 1986a, AJ 92, 131
Giménez A., de Castro E., Fernández-Figueroa M.J., 1986b, An. Fis. Ser. A 83, 349
Giménez A., Reglero V., de Castro E., Fernández-Figueroa M.J., 1987, Adv. Space Res. No. 8, 191
Grønbech B., Olsen E.H., Strömgren B., 1976, A&AS 26, 155
Hartmann L.W., Noyes R.W., 1987, ARA&A 25, 443
Nelles B., Richtler Th., Seggewiss W., 1985, in: Calibration of Fundamental Stellar Quantities, eds. D.S. Hayes, L.E. Pasinetti, A.G. Davis Phillip, IAU Symp. 111, p. 499
Nissen P.E., Twarog, B.A., Crawford D.L., 1987, AJ 93, 634
Olsen E.H., 1984, A&AS 57, 443
Olsen E.H., 1988, A&A 189, 173
Olson E.C., 1974, AJ 79, 1424
Petersen B.R., 1982, in: Activity in Red Dwarf Stars, eds. P.D. Byrne, M. Rodonò, IAU Coll. No. 71, Reidel, Dordrecht, p. 17
Popper D.M., 1990, AJ 100, 247
Reglero V., Giménez A., de Castro E., Fernández-Figueroa M.J., 1987, A&AS 71, 421
Reglero V., Giménez A., Estela A., 1990, A&A 231, 375
Rucinski S., 1981, Acta Astron. 31, 409
Saxner M., Hammarback G., 1985, A&A 151, 372
Schuster W.J., Nissen P.E., 1989, A&A 221, 65
Strassmeier, K.G., Hall D.S., Zeilik M., Nelson E., Eker Z., Fekel F.C., 1988, A&AS 72, 291
Strömgren B., 1966, ARA&A 4, 443